

1 **An Interactive Tool to Forecast US Hospital Needs in the Coronavirus 2019 Pandemic**

2

3 Kenneth J. Locey^{1*}, Thomas A. Webb^{1**}, Jawad Khan^{2***}, Anuja K. Antony^{3†}, Bala Hota^{1,3,4††}

4

5 **Affiliations**

6 ¹ Center for Quality, Safety and Value Analytics, Rush University Medical Center, Chicago,
7 Illinois, 60612, USA.

8 ² Knowledge Management Services, Rush University Medical Center, Chicago, Illinois, 60612,
9 USA.

10 ³ Department of Surgery, Division of Plastic and Reconstructive Surgery, Rush University
11 Medical Center, Chicago, Illinois, 60612, USA.

12 ⁴ Department of Internal Medicine, Division of Infectious Diseases, Rush Medical College,
13 Chicago, Illinois, 60612, USA.

14

15 * Corresponding author. email: Kenneth_J_Locey@rush.edu

16 **Coauthor Contact emails**

17 ** Thomas_A_Webb@rush.edu

18 *** Jawad_Khan@rush.edu

19 † Anuja_K_Antony@rush.edu

20 †† Bala_Hota@rush.edu

21

22

23

24

25

26

27

28

29

30

31

ABSTRACT

Hospital enterprises have been continually faced with anticipating the spread of COVID-19 and the effects it is having on visits, admissions, bed needs, and crucial supplies. While many studies have focused on understanding the basic epidemiology of the disease, few open source tools have been made available to aid hospitals in their planning. We developed a web-based application (available at: <http://covid19forecast.rush.edu/>) for US states and territories that allows users to choose from a suite of models already employed in characterizing the spread of COVID-19. Users can obtain forecasts for hospital visits and admissions as well as anticipated needs for ICU and non-ICU beds, ventilators, and personal protective equipment supplies. Users can also customize a large set of inputs, view the variability in forecasts over time, and download forecast data. We describe our web application and its models in detail and provide recommendations and caveats for its use. Our application is primarily designed for hospital leaders, healthcare workers, and government official who may lack specialized knowledge in epidemiology and modeling. However, specialists can also use our open source code as a platform for modification and deeper study. As the dynamics of COVID-19 change, our application will also change to meet emerging needs of the healthcare community.

INTRODUCTION

60
61
62
63
64
65
66
67
68
69
70
71
72
73
74
75
76
77
78
79
80
81
82
83
84
85
86
87
88
89
90

Coronavirus disease 2019 (COVID-19) was declared a global pandemic by the World Health Organization on March 11th 2020. By then, confirmed COVID-19 cases were reported among 109 countries and exceeded 128,000 worldwide (data source: Johns Hopkins University Center for Systems Science and Engineering). That number increased more than 10-fold in less than one month. As COVID-19 spreads within and among nations, healthcare enterprises grapple with the challenges of preparing for the growing number of COVID-19 patients and with appropriating the resources needed to treat patients while protecting healthcare professionals. In the United States (US), policy makers and hospital leaders prognosticate on how to best allocate resources in the face of an anticipated surge in demand that may last for several months to come (Bukhari and Jameel, 2020). However, even as COVID-19 threatens to overwhelm healthcare systems, the predictive analytics tools that would otherwise allow hospitals to make informed decisions are lagging behind the increasing number of studies aimed at characterizing the basic epidemiology of COVID-19.

To meet the pressing needs of hospital enterprises we developed an interactive, open-source web-based application to provide state- and hospital-specific forecasts of COVID-19 patients and related supplies. Our application is available on the <http://covid19forecast.rush.edu/> website and allows users to employ a suite of models already used in the prediction of COVID-19 cases. It then couples these models to granular customizable inputs to produce hospital-level forecasts for COVID-19 visits and admits, ICU and non-ICU beds, ventilators, and various personal protective equipment (PPE) supply needs. Our efforts are aimed at addressing immediate and anticipated healthcare demands, and to allow informed decision-making by government officials and healthcare professionals who may lack specialized expertise in epidemiology, modeling, and data science. By making our aggregated data and source code freely available, and by offering additional source code outside the application itself, epidemiologists, modelers, and data scientists may also find our application useful as is, or as a modifiable resource for deeper analysis.

In this paper, we describe our application in detail, focusing on the data and models it uses, the inputs it allows users to enter, and the graphs, tables, and downloadable data it provides. We also provide guidance on the use of this application, the interpretation of its

91 outputs, and the caveats of our approach. Finally, we discuss the value of our application to
92 meeting the needs of the healthcare community, its potential as a tool for generating novel
93 insights, and modifications to come. In addition to our aim of empowering administrators,
94 physicians, and governmental agencies to make informed decisions, we sought to enable other
95 predictive healthcare analytics teams and researchers. Specifically, the modification and
96 deployment of our application's source code requires a minimal set of widely popular open
97 source software (e.g., python language, Jupyter notebook) and little-to-no experience in web
98 development.

99

100

101

FUNCTIONALITY AND USE

102

103 **Overview** – Our open-source application allows users 1) to aggregate data from a popular open-
104 source repository of COVID-19 data, 2) to track and forecast the progression of COVID-19 cases
105 across US states using a suite of well-known models, 3) customize a large set of input parameters
106 to provide state- and hospital-specific forecasts for numbers of hospital visits, admitted patients,
107 ICU needs, and personal protective equipment (PPE) supply needs. The application also allows
108 users to adjust the length of forecasts, to adjust expected time lags in patient visits, to adjust the
109 average length of stay (LOS) for ICU and non-ICU patients, to examine forecasts from previous
110 days, and to download forecast data for deeper analysis.

111

112 **Data** – Our application accesses COVID-19 data from the Johns Hopkins University Center for
113 Systems Science and Engineering (JHU CSSE) (2). Specifically, our application downloads,
114 aggregates, and stores daily reports from the JHU CSSE public GitHub repository
115 (<https://github.com/CSSEGISandData/COVID-19>). These daily reports contain cumulative
116 numbers of confirmed cases, and cumulative numbers of reported deaths and recoveries for
117 counties, states, provinces, and nations reported since January 22nd, 2020. For select models, our
118 application uses population sizes for US states and territories based on data from the US Census
119 Bureau (2010 – 2019). Our application also uses dates of COVID-19 arrival in US states and
120 territories based on data available from state and territory governmental agencies (e.g.,
121 Departments of Health).

122

123 **Modeling COVID-19 cases** – Our application begins by modeling the cumulative COVID-19
124 cases for a selected state, and allows users to choose from four simplistic models of growth that
125 have been used in characterizing the spread of COVID-19 as well as one popular
126 epidemiological model that has been frequently used in the study of COVID-19 (Fig 1).
127 Altogether, the following suite of models allows users the ability to compare and contrast
128 forecasts resulting from different forms of growth and varying complexity of disease dynamics
129 and social response (e.g., testing lags, social distancing).

130

131 *Exponential growth* – Initial stages of growth often appear limited only by the inherent growth
132 rate (r) of the population or disease. In this way, exponential growth proceeds multiplicatively
133 according to a simple functional form, $N_t = N_0 e^{rt}$, where N_0 is the initial infected population size,
134 t is the amount of passed, and N_t is the infected population size at t . The exponential model has
135 been widely used to characterize the spread of COVID-19 the during initial weeks of infection
136 (e.g., Graselli, Presenti, and Cecconi 2020, Lui *et al.* 2020, Remuzzi and Remuzzi, 2020; Fig 2).
137 Because it assumes that r is constant, the exponential model has a simple log-linear
138 transformation, $\log(N_t) = \log(N_0) + t \cdot r$, that allows log-transformed numbers of cases to be
139 regressed on t (Sit, Poulin-Costello, and Bergerud 1994). Our application uses this exponential
140 regression to obtain predictions for the expected cumulative number of confirmed COVID-19
141 cases (N). This model has explained upwards of 99% of variation in the initial days or weeks of
142 COVID-19 spread within states; however, it quickly begins to fail because it only allows for
143 continued rapid growth (Fig 2).

144

145 *Quadratic growth* – Initial stages of growth may be more rapid than that expected from the
146 exponential model while the latter monotonic increase in N can proceed less rapidly than
147 predicted by the exponential. In these cases, growth may be quadratic, i.e., characterized by a
148 constant change in growth rate. Early COVID-19 studies have implicated quadratic growth in
149 spread of COVID-19 (e.g., Brandenburg 2020; Fang, Ne, and Penny 2020) and the quadratic
150 model, to date, has continued to perform well (Fig 2). The quadratic function, $f(x) = x^2 + x + c$, is
151 a 2nd order polynomial that can be applied to population growth as $N_t = \beta_1 t^2 + \beta_2 t + N_0$. Our
152 application uses numerical optimization of the fitted parameters, β_1 and β_2 , to find the best fit

153 quadratic function for a given time series and hence, to predict values for (N). This model has,
154 thus far, improved as COVID-19 spreads and has explained upwards of 99% of variation in
155 COVID-19 cases among states (Fig 2). However, like the exponential model, the quadratic
156 model only allows for continued growth, i.e., no saturation. Consequently, the quadratic model
157 must eventually fail as COVID-19 cases saturate.

158
159 *Logistic growth* – Exponential growth within a population cannot continue *ad infinitum*. Instead,
160 growth must slow as an upper limit is approached or as natural limitations to disease spread (e.g.,
161 immunity, contact among hosts) are encountered. The logistic model captures this slowing and
162 eventual saturation, resulting in a sigmoidal or s-shaped growth curve (Maynard-Smith 1978,
163 Bacaër 2011, Fig 1). In addition to exponential and quadratic growth, early COVID-19 studies
164 have implicated logistic growth in the spread of the disease (Roosa *et al.* 2020, Wu *et al.* 2020).
165 Like the quadratic model, the logistic model has also continued to perform well as states have
166 progressed in COVID-19 infection (Fig 2). The logistic model takes a relatively simple
167 functional form, $N_t = \frac{\alpha}{1+e^{-rt}}$, where α is the upper limit of N and r is the intrinsic rate of
168 increase. Our application uses numerical optimization of α and r to find the best fit logistic
169 function and hence, predicted values for N . This model has, to date, improved as COVID-19
170 spreads and has explained upwards of 99% of variation in COVID-19 cases among states (Fig 2).

171
172 *Gaussian growth* – The Gaussian (i.e., normal) distribution can provide a relatively simple and
173 close approximation to complex epidemiological models (Buckingham-Jeffery *et al.* 2018):

$$f(x) = \frac{1}{\sigma\sqrt{2\pi}} e^{-\frac{1}{2}\left(\frac{x-\mu}{\sigma}\right)^2}$$

174
175
176
177 This symmetrical curve has two parameters, mean = μ , standard deviation = σ , and belongs to the
178 family of exponential distributions (Fig 1). When used to model spread of disease, Gaussian
179 curves are symmetrical around a climax day with the change in the rate of growth determining
180 the standard deviation about the curve. Gaussian models have previously been successful in
181 approximating the spread of COVID-19 in Germany (Schlickeiser and Schlickeiser 2020). Our
182 application uses numerical optimization of μ and σ and the cumulative distribution function of

183 the Gaussian model to find the best fit cumulative Gaussian function and hence, predicted values
184 for N . This model has, thus far, explained >99% of variation in COVID-19 cases among states
185 and continues to improve as COVID-19 spreads (Fig 2).

186

187 *SEIR-SD* – To date, COVID-19 studies have used a variety of epidemiological models to
188 characterize the spread of the disease within populations. The modeling in several of these
189 studies has been based on refinements to the classic SEIR model of Hethcote and Tudor (1980)
190 (see Boldog *et al.* 2020, Peng *et al.* 2020, Lui *et al.* 2020, Wang *et al.* 2020). In this model, a
191 contagious disease drives changes in the fraction of susceptible persons (S), the fraction of
192 persons exposed but not yet exhibiting infection (E), the fraction of infectious persons (I), and
193 the fraction of persons recovered (R), where $S + E + I + R = 1$. These SEIR subpopulations are
194 modeled as compartments in the following set of ordinary differential equations:

195

$$196 \quad \frac{dS}{dt} = \beta SI, \quad \frac{dE}{dt} = \beta SI - \alpha E$$

197

$$198 \quad \frac{dI}{dt} = \alpha E - \gamma I, \quad \frac{dR}{dt} = \gamma I$$

199

200 In these equations, α is the inverse of the incubation period, and γ is the inverse of the average
201 infectious period, and β is the average number of contacts of infected persons with susceptible
202 persons per unit time. Our application imputes the initial value of β from a well-known
203 simplifying relationship between γ and the basic reproductive number (R_0), i.e., $\beta = \gamma R_0$
204 (Ridenhour *et al.* 2018, Rocklöv *et al.* 2020, Rădulescu and Cavanagh 2020, Lin *et al.* 2020).

205 We allowed β to decrease in proportion to I . We assumed that people will, on average,
206 reduce their contact with others when the populace is aware that an increasing percent of their
207 population is infected. This approach allows an inherent degree of social distancing to emerge as
208 a frequency-dependent phenomenon. We also simulated an explicit effect of social distancing (λ)
209 to capture the overall strength of response to public health policies. These effects were included
210 as time-iterative modifications to β :

$$211 \quad \beta_{t+1} = \frac{\beta_t}{\lambda I + 1}$$

212

213 This function allows β to remain unchanged when either I or λ equal 0. When λ equals 1, the
214 daily change in β is governed by the implicit frequency-dependent effect of I . Importantly,
215 simple algebraic rearrangement shows that the product of social distancing (λ) and the fraction
216 infected (I) determines the percent daily change in contact rate (β):

217

$$218 \quad \lambda I + 1 = \frac{\beta_t}{\beta_{t+1}}$$

219

$$220 \quad \lambda \cdot 100 \cdot I = 100 \cdot \frac{\beta_t - \beta_{t+1}}{\beta_{t+1}}$$

221

222 As a result, λ determines the daily proportional change in the contact rate per infected fraction of
223 the total population:

$$224 \quad \lambda = \frac{\beta_t - \beta_{t+1}}{I\beta_{t+1}}$$

225

226 We also modified the classic SEIR model to account for initial time lags in COVID-19
227 testing. Specifically, and particularly in the US, widespread testing for COVID-19 may have
228 artificially dampened the apparent number of positive cases within the first month of the first
229 reported infection. We accounted for this effect by modifying the apparent size of I while
230 allowing the actual size of I to grow according to the SEIR-SD dynamic. This time-iterative
231 modification took the following logistic functional form:

232

$$233 \quad I_t \frac{1}{1 + e^{-\tau t + \varepsilon}},$$

234

235 where τ and ε are fitted parameters. This equation models testing as low-to-nonexistent during
236 the initial weeks of outbreak, and then accelerates afterwards.

237

238 To date, the SEIR-SD model has generally performed as well as or better than the
239 exponential, quadratic, logistic, and gaussian models (Fig 2). Our application performs a pseudo-
optimization on the SEIR-SD model parameters and a likely date of initial infection, as opposed

240 to using the first reported occurrence. Our implementation of the SEIR-SD model is based on an
241 unbiased search of multivariate parameter space within ranges of parameter values derived from
242 population sizes for US states and territories and the increasing corpus of COVID-19 literature
243 (Table 1). Our application performs 50,000 iterations and chooses the set of parameters that
244 maximize the explained variation in observed data. This implementation avoids the
245 computational challenges of applying numerical optimizers to complex simulation models and
246 avoids the problems that these optimizers can have in becoming trapped in local minima.

247

248 ***Forecasting COVID-19 cases*** – Our application allows users to select one of the above-
249 mentioned models and a location from a list of US states and territories (Fig 3). It then plots the
250 reported number of cumulative COVID-19 cases along with model predictions (up to present
251 day) and forecasts (up to 60 days ahead) (Fig 3). Users can also view how the predictions and
252 forecasts have changed over the last 10 days (Fig 3).

253

254 ***Forecasting hospital visits and admits via time lags*** – Our application allows users to enter the
255 expected percent of state-wide COVID-19 cases that visit their hospital as well as the expected
256 percent of those admitted. Going further, we accounted for the tendency of infected persons to
257 not seek immediate medical attention. We modeled these time lags as Poisson distributed random
258 variables, whereby portions of newly infected patients may wait 1, 2, 3, ..., days to visit the
259 hospital. The Poisson distribution has ideal properties for modeling this scenario. Specifically, it
260 is a discrete probability distribution (x -values correspond to days) with a simplistic formulation
261 (e.g., the mean equals the variance), where the only parameter needed to obtain the probability
262 mass function (i.e., mean), directly corresponds to the expected average time lag. Users can view
263 the change in the forecasted patient census by adjusting the expected time lag (Fig 4).

264

265 ***Forecasting hospital bed and ICU needs via daily carry-over*** – Our application allows users to
266 forecast the number of hospital beds, ICU beds, and ventilators needed. The user begins by
267 entering expected values for the percent of COVID-19 patients admitted to critical care, the
268 expected average length of stay (LOS) for ICU and non-ICU patients, as well as the expected
269 percent of ICU patients on ventilators. The application then uses these inputs to calculate the
270 fraction of newly admitted ICU, non-ICU, and ICU-ventilator patients expected each day.

271 Because bed needs must also reflect the numbers of beds needed for new admissions, those
272 opened from discharges, and those currently occupied, our application models the daily carry-
273 over of the patient census using expected LOS and the cumulative distribution function (cdf) of
274 the binomial distribution.

275 The binomial distribution is a discrete probability distribution that models binary
276 outcomes (e.g., patients either leave the hospital or stay for an additional day) and requires only
277 two parameters (p , n). We set the value of p to 0.5 and set the value of n to be twice the average
278 LOS. Doing so produces a symmetrical probability mass function (pmf), with a mean equal to
279 the average LOS. This pmf is then converted to a cdf, which produces a first approximation for
280 the fraction of 1-day, 2-day, ..., etc., patients that are expected to be discharged on the present
281 day. The fraction of patients not expected to be discharged are then carried over to the following
282 day, e.g., a 1st-day patient becomes a 2nd-day patient and thereby has a different probability of
283 leaving the hospital on the current day. This process is then iterated from the date of the first
284 COVID-19 admit to the latest day in the user-requested forecast window (Fig 5).

285
286 ***Forecasting supply needs*** – Our application allows users to forecast personal protective
287 equipment (PPE) needs in accordance with the forecasted census of COVID-19 ICU, non-ICU,
288 and ICU on ventilator patients. Users can enter expected per patient per day values for surgical
289 gloves, nitrile exam gloves, vinyl exam gloves, anti-fog procedural face masks, fluid resistant
290 procedural face masks, extra-large yellow isolation gowns, anti-fog (with film) surgical face
291 masks, anti-fog full face shields, and particulate filter respirators. These values entered are then
292 multiplied by the respective patient type across the forecasted patient census to produce
293 graphical and tabulated results (Fig 6).

294
295 ***Provisioning of forecasted data*** – Our application allows users to download forecast data in .csv
296 format from each displayed table. This includes a table of forecasted cases, visits, and admits, a
297 table of ICU and non-ICU bed needs, and a table of PPE supply needs. These downloadable files
298 correspond to the model chosen by the user. Importantly, for layout purposes, the application
299 does not display rows of data beyond a 14-day forecast. Instead, the user can view data from
300 longer forecasts via the downloadable .csv files.

301

302 ***Provisioning of source code*** – Source code for our application was built using the Python
303 language (v3.7.4), Jupyter notebook, and the python-based Voila software which converts
304 Jupyter notebooks to dashboard-like applications. All code and associated data are available
305 from the public GitHub SupplyDemand repository, found on the Rush Quality Safety and Value
306 analytics GitHub organization (<https://github.com/Rush-Quality-Analytics/SupplyDemand>). The
307 repository provides an informative README.md file and the source code includes extensive
308 commenting to assist users in their use and potential modification.

309

310

DISCUSSION

311

312 ***Meeting immediate needs*** – Hospitals and healthcare enterprises are endeavoring to make
313 appropriate preparations and acquire adequate supplies to meet the challenges of the COVID-19
314 pandemic. While many studies have aimed to characterize the basic epidemiology of the disease,
315 and many online tools have been developed to visualize its spread, few tools have been
316 developed that empower hospitals to make informed decisions about expected visits and admits,
317 ICU beds, ventilator, and PPE needs. To this end, our application is already in use by our home
318 institution and several hospitals across the country and is available on the
319 <http://covid19forecast.rush.edu/> website. Consequently, the present work is intended to 1) make
320 our application broadly known to the healthcare and scientific communities 2) give healthcare
321 providers an in-depth understanding of our application, and 3) to point specialists, non-
322 specialists, and in-house predictive analytics teams to a freely available tool that can also serve
323 as modifiable platform of analytical source code and aggregated data. While some regions in the
324 United States have started to experience peaks in cases with plateaus and declines, we anticipate
325 that until a vaccine is available, episodes of repeated increased cases will be seen, for which
326 forecast models will inform operational responses.

327

328 ***Novel insights for applied and basic research*** – While our intention was not to provide *de novo*
329 models or to provide refined epidemiological parameter estimates, our tool does allow for novel
330 insights. First, our SEIR-SD model incorporates two phenomena of global, national, and local
331 concern, i.e., social distancing and lags in COVID-19 testing. To our knowledge few extensions
332 of the SEIR model have accounted for social distancing in being driven by an emergent social
333 response to increased percent infected and as driven by external forces (e.g., public policy).

334 Likewise, few if any SEIR models have accounted for the influence of lags in testing on the
335 apparent size of the infected population. Second, we envision that applied and basic research
336 studies can be conducted using the downloadable data of our application and the freely available
337 source code. Specifically, users can investigate any number of simple-to-complex relationships
338 using the downloadable forecast data that results from our suite of models and which is offered
339 alongside adjustable forecast windows, time-lags, lengths of stay, as well as other customizable
340 parameters and aggregated data (population size, date of first reported infection, numbers of
341 confirmed COVID-19 cases).

342
343 *Pending and potential modifications* – We are continually improving the functionality and
344 performance of our application to meet the predictive analytic needs of our home institution and
345 broader healthcare community. In the near future, we will include models to predict the eventual
346 decline of the pandemic and potential resurgence as social distancing guidelines and other
347 mitigating policies are relaxed. We also look to provide the functionality to 1) examine regions
348 outside the US, 2) examine county-level regions within the US, 3) include a greater array of
349 supply needs and forecasts for numbers of providers and staff needed, and 4) allow providers to
350 begin planning how and when to increase the number of elective surgeries and ambulatory visits.
351 In building our open-source application from a small set of freely available and highly popular
352 software tools, we expect that other researchers and healthcare analytics teams could readily
353 pursue these and other improvements.

354
355 *Caveats and limitations* – Our web application is versatile and easy to use. However, users
356 should consider the following caveats and limitations of modeling. First, our application draws
357 from a widely used COVID-19 dataset that may not reflect the true prevalence of COVID-19
358 within each US state and territory. While our application allows users to enter several parameters
359 (e.g., % of infected visiting one's hospital), these may change over time. Additionally, length of
360 stay for ICU and non-ICU patients likely fluctuates and may not necessarily be binomially
361 distributed. Similarly, time lags in hospital visits may not necessarily be Poisson distributed and
362 may also fluctuate across time. PPE usage rates may also fluctuate based on changing hospital
363 policies and supply shortages. Finally, our application does not account for differences in

364 susceptibility to COVID-19 with respect to age nor the influence of comorbid conditions and
365 sociodemographic factors.

366

367

ACKNOWLEDGMENTS

368 We thank the Johns Hopkins University Center for Systems Science and Engineering (JH CSSE)

369 for continuing to provide daily updated data on the COVID-19 pandemic.

370

REFERENCES

- 371
372
373 1. Anderson, R.M., Heesterbeek, H., Klinkenberg, D. and Hollingsworth, T.D. 2020. How will
374 country-based mitigation measures influence the course of the COVID-19 epidemic? *The*
375 *Lancet*. 395:931-934.
376
377 2. Brandenburg, A. 2020. Quadratic growth during the 2019 novel coronavirus epidemic. *arXiv*
378 *preprint arXiv:2002.03638*.
379
380 3. Bacaër, N. 2011. *A short history of mathematical population dynamics*. Springer Science &
381 Business Media.
382
383 4. Boldog, P., Tekeli, T., Vizi, Z., Dénes, A., Bartha, F.A. and Röst, G. 2020. Risk assessment
384 of novel coronavirus COVID-19 outbreaks outside China. *Journal of clinical*
385 *medicine*. 9:571.
386
387 5. Buckingham-Jeffery, E., Isham, V. and House, T. 2018. Gaussian process approximations for
388 fast inference from infectious disease data. *Mathematical biosciences*. 301:111-120.
389
390 6. Bukhari, Q. and Jameel, Y. 2020. Will coronavirus pandemic diminish by
391 summer? Available at: <http://dx.doi.org/10.2139/ssrn.3556998>.
392
393 7. Cao, Z., Zhang, Q., Lu, X., Pfeiffer, D., Jia, Z., Song, H. and Zeng, D.D. 2020. Estimating the
394 effective reproduction number of the 2019-nCoV in China. medRxiv:
395 2020.01.27.20018952; doi: <https://doi.org/10.1101/2020.01.27.20018952>.
396
397 8. Fang, Y., Nie, Y. and Penny, M. 2020. Transmission dynamics of the COVID-19 outbreak
398 and effectiveness of government interventions: A data-driven analysis. *Journal of*
399 *medical virology*. 92:645-659.
400
401 9. Hethcote, H.W. and Van den Driessche, P. 1991. Some epidemiological models with
402 nonlinear incidence. *Journal of Mathematical Biology*. 29:271-287.
403
404 10. Grasselli, G., Pesenti, A. and Cecconi, M. 2020. Critical care utilization for the COVID-19
405 outbreak in Lombardy, Italy: early experience and forecast during an emergency
406 response. *Jama*. doi:10.1001/jama.2020.4031.
407
408 11. Johns Hopkins University Center for Systems Science and Engineering, 2019 Novel
409 Coronavirus COVID-19 (2019-nCoV) Data Repository.
410 <https://github.com/CSSEGISandData/COVID-19>.
411

- 412 12. Kucharski, A.J., Russell, T.W., Diamond, C., Liu, Y., Edmunds, J., Funk, S., Eggo, R.M.,
413 Sun, F., Jit, M., Munday, J.D. and Davies, N. 2020. Early dynamics of transmission and
414 control of COVID-19: a mathematical modelling study. *The Lancet Infectious Diseases*.
415 [https://doi.org/10.1016/S1473-3099\(20\)30144-4](https://doi.org/10.1016/S1473-3099(20)30144-4).
416
- 417 13. Lin, Q., Zhao, S., Gao, D., Lou, Y., Yang, S., Musa, S.S., Wang, M.H., Cai, Y., Wang, W.,
418 Yang, L. and He, D. 2020. A conceptual model for the coronavirus disease 2019
419 (COVID-19) outbreak in Wuhan, China with individual reaction and governmental
420 action. *International journal of infectious diseases*. 93:211-216.
421
- 422 14. Liu, Y., Gayle, A.A., Wilder-Smith, A. and Rocklöv, J. 2020. The reproductive number of
423 COVID-19 is higher compared to SARS coronavirus. *Journal of travel medicine*. 22:1-4.
424 <https://doi.org/10.1093/jtm/taaa021>
425
- 426 15. Locey, K.J. and White, E.P. 2013. How species richness and total abundance constrain the
427 distribution of abundance. *Ecology letters*. 16:1177-1185.
428
- 429 16. Pedersen, M.G. and Meneghini, M. 2020. Quantifying undetected COVID-19 cases and
430 effects of containment measures in Italy. *ResearchGate Preprint* (online 21 March 2020)
431 DOI. 2020;10.
432
- 433 17. Maier, B.F. and Brockmann, D. 2020. Effective containment explains sub-exponential
434 growth in confirmed cases of recent COVID-19 outbreak in Mainland China. *arXiv*
435 preprint arXiv:2002.07572.
436
- 437 18. Maynard-Smith, J. 1978. *Models in ecology*. Cambridge University Press. Cambridge.
438
- 439 19. Peng, L., Yang, W., Zhang, D., Zhuge, C. and Hong, L. 2020. Epidemic analysis of COVID-
440 19 in China by dynamical modeling. *arXiv preprint arXiv:2002.06563*.
441
- 442 20. Read, J.M., Bridgen, J.R., Cummings, D.A., Ho, A. and Jewell, C.P. 2020. Novel
443 coronavirus 2019-nCoV: early estimation of epidemiological parameters and epidemic
444 predictions. *MedRxiv*. doi: <https://doi.org/10.1101/2020.01.23.20018549>
445
- 446 21. Remuzzi, A. and Remuzzi, G. 2020. COVID-19 and Italy: what next? *The Lancet*. doi:
447 [https://doi.org/10.1016/S0140-6736\(20\)30627-9](https://doi.org/10.1016/S0140-6736(20)30627-9)
448
- 449 22. Ridenhour, B., Kowalik, J.M. and Shay, D.K. 2018. Unraveling R 0: Considerations for
450 Public Health Applications. *American journal of public health*. 108:S445-S454.
451

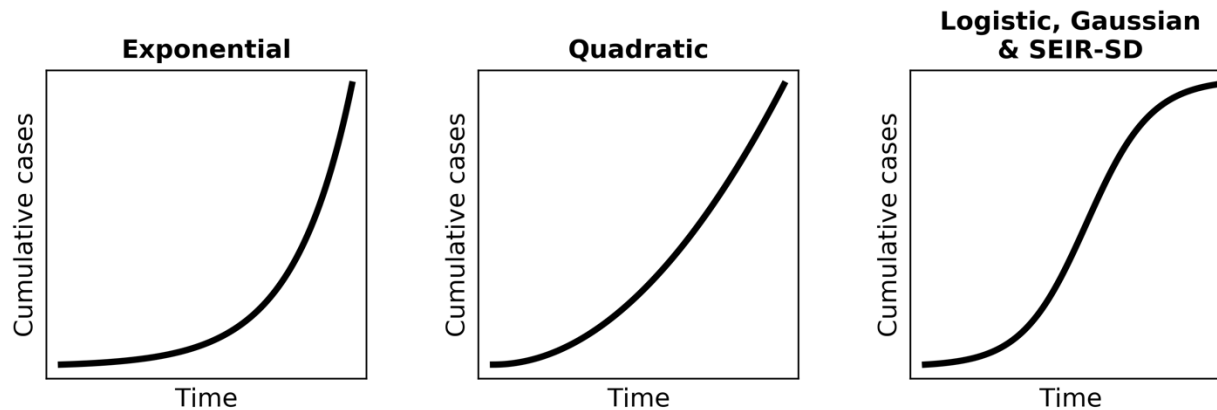
- 452 23. Rocklöv, J., Sjödin, H., Wilder-Smith, A. 2020. COVID-19 outbreak on the Diamond
453 Princess cruise ship: estimating the epidemic potential and effectiveness of public health
454 countermeasures. *Journal of travel medicine*. doi: <https://doi.org/10.1093/jtm/taaa030>
455
- 456 24. Roosa, K., Lee, Y., Luo, R., Kirpich, A., Rothenberg, R., Hyman, J.M., Yan, P. and Chowell,
457 G. 2020. Real-time forecasts of the COVID-19 epidemic in China from February 5th to
458 February 24th, 2020. *Infectious Disease Modelling*. 5: 256-263.
459
- 460 25. Sit, V., Poulin-Costello, M. and Bergerud, W. 1994. *Catalogue of curves for curve fitting*.
461 Forest Science Research Branch, Ministry of Forests.
462
- 463 26. Wang, H., Wang, Z., Dong, Y., Chang, R., Xu, C., Yu, X., Zhang, S., Tsamlag, L., Shang,
464 M., Huang, J. and Wang, Y. 2020. Phase-adjusted estimation of the number of
465 coronavirus disease 2019 cases in Wuhan, China. *Cell Discovery*. 6:1-8.
466
- 467 27. WHO Director-General's opening remarks at the media briefing on COVID19 -March 2020.
468 [https://www.who.int/dg/speeches/detail/who-director-general-s-opening-remarks-at-the-](https://www.who.int/dg/speeches/detail/who-director-general-s-opening-remarks-at-the-media-briefing-on-covid-19---11-march-2020)
469 [media-briefing-on-covid-19---11-march-2020](https://www.who.int/dg/speeches/detail/who-director-general-s-opening-remarks-at-the-media-briefing-on-covid-19---11-march-2020).
470
- 471 28. Wu, K., Darcet, D., Wang, Q. and Sornette, D. 2020. Generalized logistic growth modeling
472 of the COVID-19 outbreak in 29 provinces in China and in the rest of the world. arXiv
473 preprint arXiv:2003.05681.
474
- 475 29. You, C., Deng, Y., Hu, W., Sun, J., Lin, Q., Zhou, F., Pang, C.H., Zhang, Y., Chen, Z. and
476 Zhou, X.H. 2020. Estimation of the time-varying reproduction number of COVID-19
477 outbreak in China. *Available at SSRN 3539694*.

478 **Table 1.** Biological parameters for the SEIR-SD model. Our application attempts to optimize the
479 following SEIR-SD parameters within ranges of reported values for the average incubation
480 period, the average infectious period, and the basic reproductive number.
481

Parameter	Description	Reported Range	References
Avg. Incubation period (latent period)	Days during which an infected individual cannot infect others.	5 – 6 days	Anderson <i>et al.</i> 2020 Pederson and Meneghini 2020 Wang <i>et al.</i> 2020 Kucharski <i>et al.</i> 2020 Cao <i>et al.</i> 2020
Avg. Infectious period	Days over which an infected person remains infective.	1.6 – 13 days	You <i>et al.</i> 2020 Maier and Brockmann 2020 Wang <i>et al.</i> 2020 Read <i>et al.</i> 2020
Basic Reproductive Number (R_0)	Average number of secondary infections generated by a primary infection at the onset of outbreak	2.1 – 6.5	You <i>et al.</i> 2020 Pederson and Meneghini 2020 Maier and Brockmann 2020 Wang <i>et al.</i> 2020 Lui <i>et al.</i> 2020

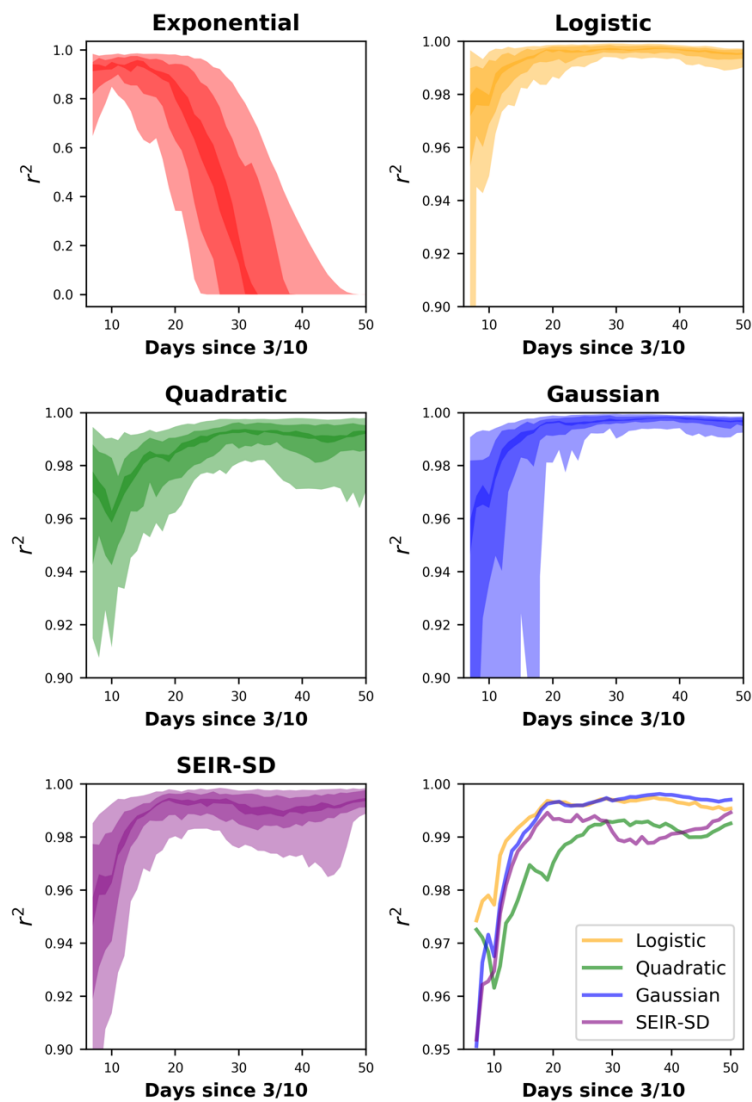
482
483
484

485 **Figure 1.** Our application allows users to choose from five models that have previously been
486 employed in the study of COVID-19, the general cumulative forms of which are depicted below.
487 While the exponential and quadratic (2nd degree polynomial) models only allow for continued
488 increase in cumulative cases, the logistic, Gaussian, and SEIR-SD models allow cumulative
489 cases to saturate.
490



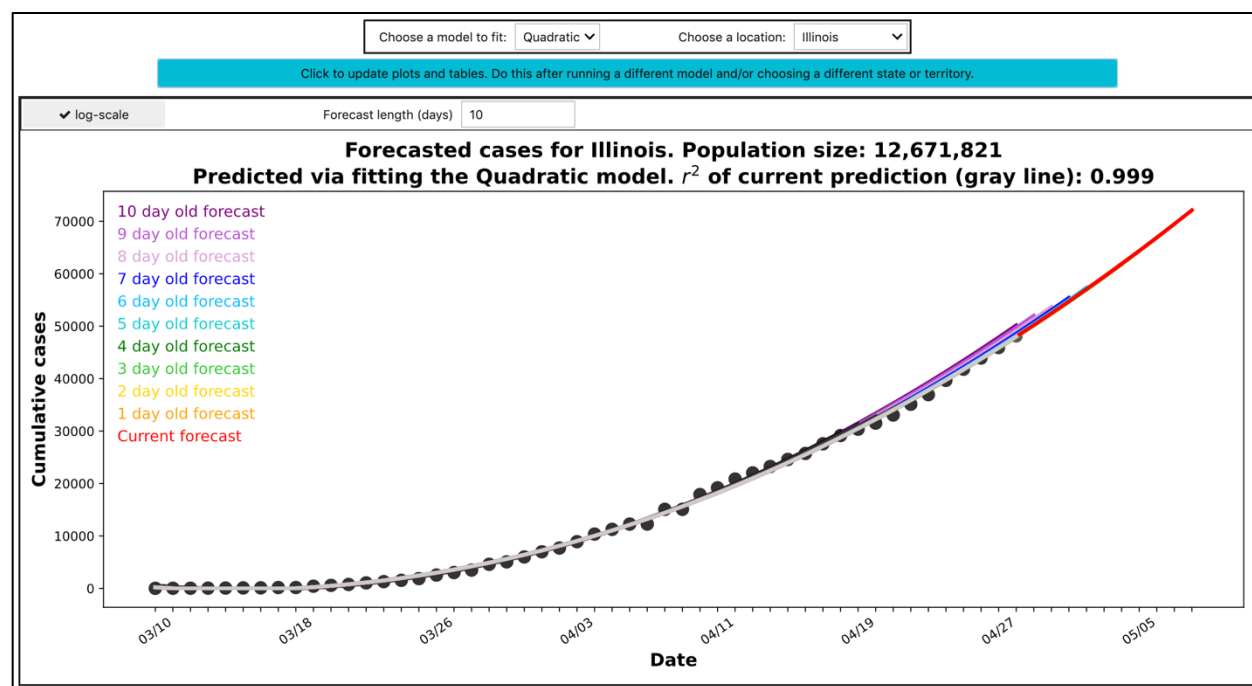
491
492
493
494

495 **Figure 2.** Confidence interval (CI) hulls for the performance of models across US states and
496 territories from March 16th to April 15th. The Johns Hopkins University Center for Systems
497 Science and Engineering (JH CSSE) data shows most states beginning to report COVID-19 cases
498 by March 10th and we allowed the models a week of data before fitting them. The x -axis is in
499 days since the first reported case, occurring on or after March 10th. Lightly colored hulls are
500 90% CI, hulls of intermediate darkness are 50%, and the darkest hulls are 10% CI. Performance
501 is measured via a modified r^2 of observed versus predicted values where the y -intercept is forced
502 through 0 (*sensu* Locey and White 2013). The y -axes are scaled to show the greatest resolution
503 for each model and are not scaled similarly across all models. Lower right: Mean r^2 values
504 among states for all models except the exponential. This figure reveals the accuracy of models
505 fitted to observed data, but do not pertain to the accuracy of future forecasts.



507 **Figure 3.** The top pane of the application features the ability to choose a location and one of four
508 models for fitting data (black dots) and for making forecasts. The user then clicks a teal button to
509 update the application's plots of fitted predictions (gray-scale lines) and forecasts (colored lines).
510 The application allows the user to extend the forecast window to 60 days and view
511 logarithmically transformed data. The current image is the result of fitting the quadratic model to
512 Illinois COVID-19 data and includes a forecast window of 10 days. Forecasts up to 10 days old
513 are displayed to aid users in examining forecast variability. Values for coefficients of
514 determination (r^2) pertain to observed versus predicted values, where the y -intercept is forced
515 through 0 (*sensu* Locey and White 2013).

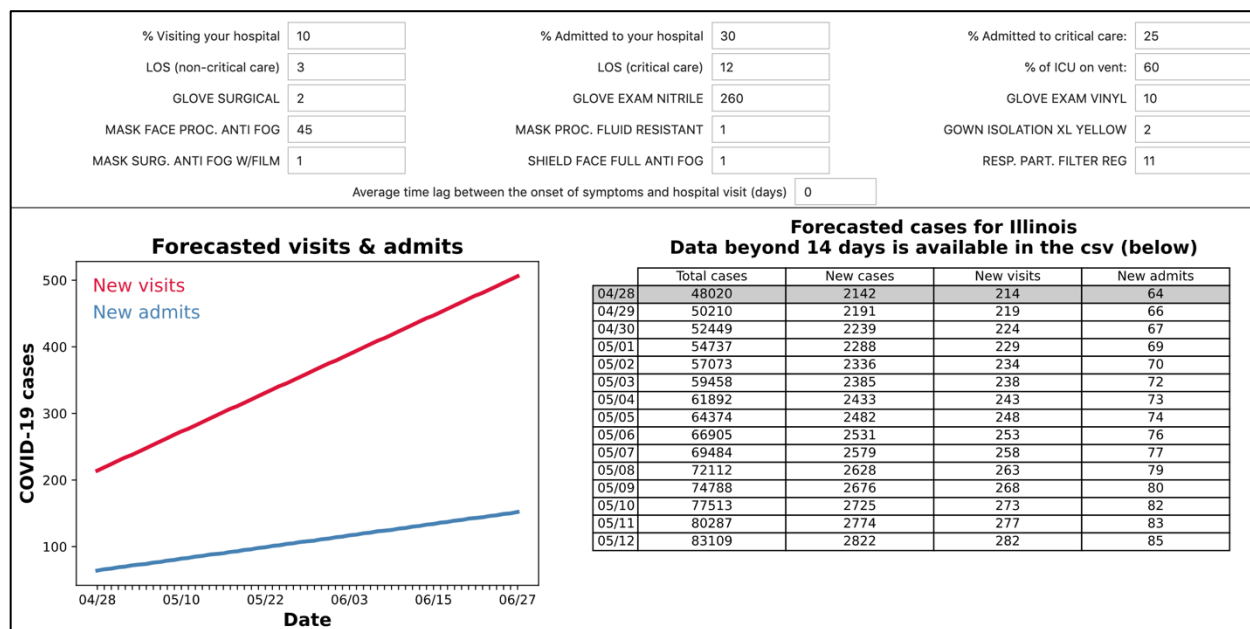
516
517



518
519
520
521

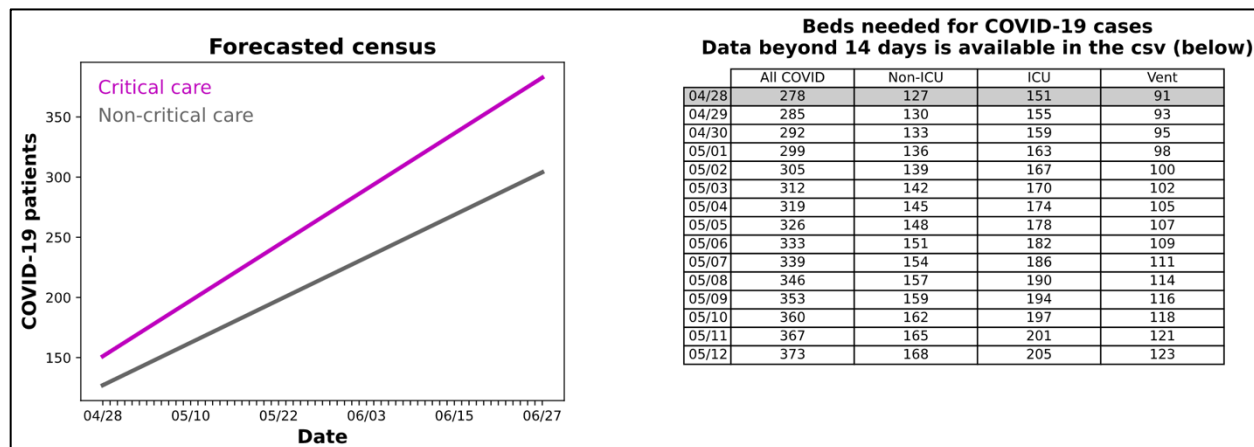
522 **Figure 4.** The second pane of our application allows users to set values for the percent of
 523 COVID-19 patients in a given state visiting their hospital, the percent admitted, and the percent
 524 admitted to critical care. Users can also enter the expected length of stay (LOS) for critical
 525 patients (ICU), non-critical care patient, the percent of ICU patients expected to be on
 526 ventilators, values for various PPE supply needs, and an expected time lag between when
 527 patients first experience symptom and when they visit the hospital. The application then plots the
 528 forecasted numbers of new visits and new admits, and then tabulates the forecasted total cases,
 529 new cases, new visits, and new admits. See figures 4 and 5 for plots and tables of patient census
 530 and PPE needs. The application informs the user that forecasted data beyond 14 days are
 531 available via csv downloads.

532
 533



534
 535
 536
 537

538 **Figure 5.** The third pane our application plots and tabulates the forecasted patient census. Left:
539 A graph of forecasted numbers of critical care and non-critical care patients. Right: A table of
540 forecasted bed needs for all COVID-19 patients, non-ICU patients, ICU patients, and ICU
541 patients on ventilators. The application informs the user that forecasted data beyond 14 days are
542 available via csv downloads.
543



544
545
546
547
548
549
550

551 **Figure 6.** The bottom pane of our application plots and tabulates forecasted PPE needs. Left:
 552 Forecasted PPE needs are plotted to reveal overall expected trends. PPE supplies with similar
 553 input values become plotted on top of each other. Right: Forecasted PPE are tabulated with color
 554 coding that corresponds to the figure on the left, to allow easier visual interpretation. The
 555 application informs the user that forecasted data beyond 14 days are available via csv downloads.
 556 Users can click the teal button at the bottom to display or refresh downloadable csv files.
 557



558